A Dynamic SEIR Approach to Foliar Disease Management in Wheat: Linking Fungicide Timing to Epidemic Growth Rate Suppression

IOANNIS VAGELAS
Department of Agriculture Crop Production and Rural Environment,
University of Thessaly, Volos,
GREECE

Abstract: - Wheat foliar diseases such as Zymoseptoria tritici and Pyrenophora triticirepentis pose significant threats to yield under Mediterranean conditions. We developed a biologically informed SEIR (Susceptible–Exposed–Infectious–Removed) model to quantify epidemic dynamics during the critical BBCH 37 growth stage and to evaluate the impact of fungicide strategies on the instantaneous epidemic growth rate r(t). The model integrates pathogenspecific traits, environmental modulation of transmission, and fungicide decay to simulate daily infection pressure over a 10day period. Scenario A (seed treatment with Systiva®) resulted in transient positive r(t) values for Z. tritici and nearzero or slightly negative values for P. triticirepentis, indicating partial suppression. Scenario B (seed treatment plus foliar propiconazole) produced consistently negative r(t) for both pathogens, reflecting stronger and sustained epidemic decline. These findings align with field data from Thessaly, Greece, and demonstrate that combining systemic seed protection with a BBCH 37timed foliar application enhances disease suppression by reducing transmission and increasing removal rates. The SEIR framework provides a practical and interpretable tool for assessing fungicide efficacy, supporting integrated disease management decisions in Mediterranean wheat systems.

Key-Words: - SEIR epidemiological modeling; Wheat leaf diseases; Pyrenophora tritici-repentis; Zymoseptoria tritici; Fungicide management strategies; Epidemic growth rate r(t); BBCH 37; Mediterranean wheat systems

Received: March 19, 2026. Revised: April 21, 2026. Accepted: June 13, 2026. Published: July 9, 2026.

1 Introduction

Wheat (Triticum aestivum) is a major crop in Mediterranean agriculture, yet its productivity is frequently constrained by foliar fungal diseases. Tan spot and Septoria leaf blotch are among the most damaging, caused by the necrotrophic pathogen Pyrenophora tritici‑repentis and the hemibiotrophic Zymoseptoria tritici, respectively [1], [2]. Their epidemiology is strongly shaped by environmental conditions: P. tritici‑repentis thrives under high humidity and moderate temperatures [3], whereas Z. tritici is highly sensitive to moisture and exhibits reduced virulence at elevated temperatures [4]. Both pathogens depend on rainfall for dispersal, and their severity increases with prolonged leaf wetness [5], [6]. Sub‑humid Mediterranean climates therefore favor their co‑occurrence, while climate change is expected to further influence their virulence and spread [4].

Crop canopy structure also plays a critical role in epidemic development. Traits such as stem height, elongation rate, and leaf size influence microclimate and pathogen dispersal [7], [8]. Dense canopies during stem elongation create favorable conditions for both pathogens, with P. tritici‑repentis dominating early in the season and Z. tritici becoming more prevalent toward stem elongation stage [7], [9]. Repeated cycles of lesion formation and spore release, modulated by canopy architecture and rainfall interception, drive epidemic progression [7]. Consequently, the stem‑elongation and flag‑leaf stages (BBCH 37–39) represent a critical window for disease development in Mediterranean wheat systems [1], [7].

Fungicides remain an essential component of Integrated Disease Management (IDM). Pyraclostrobin, propiconazole, tebuconazole, and azoxystrobin are effective against tan spot [10], while DMIs, SDHIs, and QoIs are commonly used against Z. tritici [11]. Applications at flag‑leaf emergence are recommended to prevent substantial yield losses [10], and multiple treatments may be required under high disease pressure [12], [13]. Given the rising incidence of both pathogens and the emergence of fungicide resistance, IDM strategies combining seed treatments, resistant cultivars, and optimized fungicide timing are increasingly important [14], [15].

In Greece, the simultaneous presence of P. tritici‑repentis and Z. tritici during BBCH 37–39 is

well documented [16]. IDM programs typically integrate pre‑planting seed treatments with phenology‑based foliar fungicide applications [1], [2], [16]. However, limited research has examined how pathogen biology, environmental drivers, and fungicide timing interact to shape early epidemic dynamics. To address this gap, we developed a time‑varying SEIR (Susceptible–Exposed–Infectious–Removed) model, a framework widely used in plant disease epidemiology and supported by recent mathematical analyses of SEIR‑type systems in plant pathology [17]. We adapted the SEIR structure to simulate daily infection dynamics during BBCH 37 under contrasting management scenarios [1], [2], [16], [18], [19], using the instantaneous epidemic growth rate r(t) as a comparative metric. Within this context, the SEIR model provides a mechanistic basis for evaluating fungicide strategies and quantifying their suppressive effects on epidemic development.

2 Materials and Methods

2.1 Biological Context and Pathogen Traits

The simultaneous interactions of the pathogens Z. tritici (Septoria leaf blotch) and P. tritici repentis (tan spot), in winter wheat, have been simulated in a study. Each has a distinct mode of nutrition, tempo of infection, and reaction to the environment where it occurs. The mode of nutrition for P. tritici repentis is necrotrophic; this means that it develops a toxin called (ToxA) that produces fast tissue necrosis [18]. The time period from infection to necrosis is approximately 2 days and under humid conditions, the pathogen's transmission occurs rapidly. Z. tritici is hemibiotrophic meaning it exhibits an asymptomatic colonization phase prior to necrotrophy. It has a longer latent time than P. tritici repentis, (3 - 5 days) with transmission occurring more readily with prolonged leaf wetness and moderate temperature [18]. SEIR model parameters directly influence the transmission rate (β), the latent rate (σ), the removal rate (γ), and the dynamic growth rate r(t) in these two diseases.

2.2 SEIR Modeling Framework

The SEIR (Susceptible–Exposed–Infectious–Removed) model is an epidemiological model that allows researchers to study the dynamics of infectious disease over time. In particular, it has been used to explore how different types of human and plant pathogens such P. tritici-repentis and Z. tritici develop over time, from the point where they infect their host, until symptoms are expressed, until they cause tissue to die, or the plant recovers.

The model partitions the host leaf area into four mutually exclusive compartments:

- S(t): Healthy tissue vulnerable to infection (Susceptible leaf area)
- E(t): Infected tissue in the latent phase, not yet infectious (Exposed, latent infections)
- I(t): Actively infected tissue capable of transmitting the pathogen (Infectious tissue)
- R(t): Necrotic or recovered tissue no longer participating in transmission (Removed/necrotic tissue)

The dynamics of these compartments are governed by a system of ordinary differential equations:

$$\frac{dS}{dt} = -\beta(t) \cdot S(t) \cdot I(t)$$

$$\frac{dE}{dt} = \beta(t) \cdot S(t) \cdot I(t) - \sigma(t) \cdot E(t)$$

$$\frac{dI}{dt} = \sigma(t) \cdot E(t) - \gamma(t) \cdot I(t)$$

$$\frac{dR}{dt} = \gamma(t) \cdot I(t)$$

where:

- β(t): Time-dependent transmission rate (dynamic transmission rate), modulated by temperature, humidity, and fungicide effects.
- σ(t): Latent rate, representing the transition from exposed to infectious tissue.
- γ(t): Removal rate, representing the rate of necrosis or recovery.

The SEIR model framework is well-suited to represent foliar diseases that have a well-defined latent period and have a strong dependence on environmental conditions for transmission success [20], [21]. This framework allows for the consideration of crop phenology (i.e., BBCH), how fungicides can impact disease dynamics, and specific plant pathogen characteristics (i.e., that different P. tritici-repentis isolates produce different necrosis-inducing effectors, and they are also highly host-specific).

The SEIR model has been demonstrated as a viable approach to modeling some wheat pathosystems, such as tan spot and Septoria blotch, where the latency and the influence of environmental factors on disease development are fundamental to understanding disease dynamics [20], [21], [22]. The SEIR structure also provides for characterizing the occurrence of the inverse gene-for-gene interaction in P. tritici-repentis when necrosis-inducing effectors interact with dominant susceptibility genes in the host [20].

2.3 Scenario Analysis and Derived Metrics

Two fungicide management scenarios were evaluated to quantify their impact on the epidemic dynamics of Z. tritici and P. tritici-repentis following the onset of the flag-leaf stage (BBCH 37). Scenario A represented seed treatment with Systiva® only, while Scenario B combined Systiva® with a foliar application of propiconazole. For each scenario, the SEIR model was simulated over a 10-day period, and the instantaneous epidemic growth rate r(t) was computed as described in Section 2.2.

To assess the overall epidemic momentum generated under each fungicide regime, we derived the cumulative epidemic pressure, defined as the time-integrated growth rate:

$$C(t) = \sum_{i=1}^{t} r(i)$$

Positive values of C(t) indicate net epidemic expansion, whereas increasingly negative values reflect progressive suppression. This cumulative metric provides a compact representation of the epidemic trajectory and was used to generate the comparative curves presented in Figure 1 and Figure 2.

All simulations were performed using identical initial conditions and parameter sets across scenarios to ensure that differences in epidemic pressure reflect only the fungicide treatments applied.

2.4 Mathematical Analysis of the SEIR Model

To strengthen the theoretical foundation of the modeling framework, we analyze the structure of the SEIR system under constant environmental conditions. This allows the derivation of equilibrium points and their local stability properties, which clarify the parameter regimes under which epidemic suppression (negative epidemic growth rate r(t)) is expected.

2.4.1 Model formulation under constant parameters

Assuming constant transmission rate β, latent rate σ, and removal rate γ, the SEIR system becomes:

$$\frac{dS}{dt} = -\beta SI,$$
$$\frac{dE}{dt} = \beta SI - \sigma E,$$
$$\frac{dI}{dt} = \sigma E - \gamma I,$$
$$\frac{dR}{dt} = \gamma I$$

The total leaf area is conserved:

$$S + E + I + R = 1.$$

2.4.2 Disease-free equilibrium (DFE)

Setting E=I=0, the disease-free equilibrium is:

$$(S*, E*, I*) = (1,0,0).$$

2.4.3 Endemic equilibrium

Assuming $I^* > 0$, we solve:

$$0 = -\beta S * I *,$$
$$0 = \beta S * I * -\sigma E *,$$
$$0 = \sigma E * -\gamma I *$$

From the second and third equations:

$$E* = \frac{\gamma}{\sigma I} *, S* = \frac{\gamma}{\beta}$$

The endemic equilibrium exists only if:

$$S* = \frac{\gamma}{\beta} < 1 \Leftrightarrow \beta > \gamma$$

This condition is equivalent to:

$$R0 = \beta/\gamma > 1.$$

2.4.4 Local stability of the disease-free equilibrium

We linearize the system around the DFE. The Jacobian matrix is:

$$J = \begin{pmatrix} 0 & 0 & -\beta \\ 0 & -\sigma & \beta \\ 0 & \sigma & -\gamma \end{pmatrix}$$

The characteristic polynomial is:

$$\lambda(\lambda + \sigma)(\lambda + \gamma) + \beta\sigma = 0$$

The dominant eigenvalue is:

$$\lambda \max = \beta - \gamma$$

Thus:

If $\beta<\gamma$ (i.e., $R_0<1$), then $\lambda max<0$ and the DFE is locally asymptotically stable.

If $\beta>\gamma$ (i.e., $R_0>1$), then $\lambda max>0$ and the DFE is unstable.

2.4.5 Mathematical Derivation of the Instantaneous Growth Rate r(t)

To justify the use of the epidemic growth rate r(t) as a diagnostic indicator of epidemic expansion or suppression, we derive it formally from the linearization of the SEIR system around the disease-free state. Consider the infectious subsystem:

$$E'(t) = \beta(t)S(t)\,I(t) - \sigma(t)E(t)$$

$$I'(t) = \sigma(t)E(t) - \gamma(t)I(t)$$

At the beginning of an epidemic, the susceptible leaf area satisfies S(t)≈S0≈1, and the infected compartments are small. Linearizing around the disease-free equilibrium (E,I)=(0,0) yields the Jacobian matrix:

$$J(t) = \begin{pmatrix} -\sigma(t) & \beta(t)s(t) \\ \sigma(t) & -\gamma(t) \end{pmatrix}$$

The instantaneous growth of infection is governed by the dominant eigenvalue λmax(t) of J(t). Solving the characteristic equation gives:

$$\lambda_{max}(t) = \frac{-(\sigma(t)+\gamma(t)) + \sqrt{(\sigma(t)-\gamma(t))^2 + 4\sigma(t)\beta(t)S(t)}}{2}$$

When the latent period is short relative to the infectious period (a common assumption in foliar pathogens), the dominant term simplifies to:

$$\lambda\max(t) \approx \beta(t)S(t) - \gamma(t)$$

We therefore define the instantaneous epidemic growth rate as:

$$r(t) = \beta(t)S(t) - \gamma(t)$$

This expression is mathematically equivalent to the dominant eigenvalue of the linearized system and determines whether infection increases or decreases:

r(t)>0: epidemic expansion,

r(t)<0: epidemic suppression.

Furthermore, the effective reproduction number follows directly:

$$Rt = \frac{\beta(t)S(t)}{\gamma(t)}, r(t) < 0 \iff Rt < 1$$

Thus, r(t) provides a rigorous, eigenvalue-based criterion for evaluating fungicide efficacy under time-varying environmental conditions.

Under constant parameters, the basic reproduction number is

$$R0 = \frac{\beta}{\gamma}$$

The condition for epidemic expansion, βS>γ, reduces to R0>1 when S≈1. In the time-varying model, the effective reproduction number is

$$Rt = \frac{\beta(t)S(t)}{\gamma(t)}$$

Using the expression for the dominant eigenvalue,

$$r(t) = \beta(t)S(t) - \gamma(t) = \gamma(t)(Rt - 1)$$

which shows that r(t)>0 if and only if Rt>1. Thus, the instantaneous growth rate and the reproduction number encode the same threshold dynamics, with r(t) providing a continuous, eigenvalue-based measure of epidemic tendency.

2.5 Initial Conditions and Seed Treatment Effects

The simulation started at BBCH stage 37, using actual field data collected during our previous research trials [1], [2], [16], [18], [19]. Untreated situations are modeled with a starting point for the Infectious compartment of I_0 = 0.05 (latent infections) and E_0 = 0.05 (permanent/remaining). If no previous necrosis occurred, the Susceptible compartment is calculated defensively as S_0 = 0.90 and R0 = 0. Treatment with Systiva (fluxapyroxad) has been shown to reduce early infection (primary spore germination and colonization) pressure by approximately 80% [23]. The result is that for an infected plant there is an Infectious compartment Introducing I_0 = 0.01, but the starting point for the ET and later stages of Ens & Create remain the same (E_0). The results of the Susceptible equations will be revised because of the first two equation's modifications to Calculate the new Susceptible value based on the variable changes introduced in calculations.

$$S_0 = 1 - E_0 - I_0 - R_0 = 0.94$$

These adjusted initial conditions are applied uniformly across both pathogens, with subsequent divergence governed by pathogen-specific parameters and environmental modulation.

2.6 Numerical Integration and Convergence Analysis

To ensure numerical accuracy and stability of the SEIR simulations, we evaluated two standard time-integration schemes: the explicit Euler method and the classical fourth-order Runge–Kutta (RK4) method. For a system of the form

$$X'(t) = F(X(t), t)$$

Euler integration updates the solution as

$$Xn + 1 = Xn + \Delta t\, F(Xn, tn)$$

with a global truncation error of order O(Δt). In contrast, the RK4 method achieves fourth-order accuracy,

$$Xn + 1 = Xn + \frac{\Delta t}{6} * (k1 + 2k2 + 2k3 + k4)$$

with global error $O(\Delta t^4)$, providing substantially improved precision for the same time step.

To verify that the numerical results are independent of the discretization, we performed a convergence analysis by halving the time step from Δt=0.1 to Δt=0.05 and Δt=0.025. The trajectories of S(t), E(t), I(t), and r(t) showed negligible differences between RK4 solutions at successive refinements, indicating numerical convergence. Euler integration produced slightly larger deviations at coarse time steps, consistent with its first-order accuracy, but converged to the RK4 solution as Δt→0.

Based on these tests, all simulations reported in this study were performed using the RK4 method with Δt=0.1, which provided a stable and accurate approximation of the SEIR dynamics under time-varying environmental conditions.

2.7 Parameter variation and local sensitivity analysis

In addition to the baseline simulations, we explored the response of the SEIR model to moderate changes in key epidemiological parameters. The transmission rate β, removal rate γ, and, where applicable, the latent rate σ were varied by ±20% around their baseline values, while keeping all other parameters fixed. For each parameter set, we recorded the peak infectious leaf area Imax, the time required for the epidemic growth rate r(t) to become negative, and the qualitative shape of r(t). These tests were designed to assess the robustness of the threshold condition β(t)S(t)>γ(t) and the stability conclusions derived in Section 2.3.

2.8 Environmental Modulation of Transmission

The effective transmission rate β(t) is dynamically modulated [24], by temperature T(t), relative humidity RH(t), and fungicide application $f_F(t)$:

$$\beta(t) = \beta_0 \cdot f_T(T(t)) \cdot f_{RH}(RH(t)) \cdot f_F(t)$$

The transmission rate β(t), is introduced in the methodology/model section as the core equation showing that transmission is not constant but depends on environmental factors and fungicide application.

Temperature Function:

$$f_T(T) = \exp\left(-\frac{(T - T_{\text{opt}})^2}{2\sigma_T^2}\right) \text{ with } T_{\text{opt}} = 22°\text{C}, \sigma_T = 4$$

This function explains how temperature around the optimum (T_{opt} = 22∘ C) influences transmission [25]. It is presented as a Gaussian response, showing that transmission decreases when temperature deviates from the optimum.

Humidity Function:

$$f_{RH}(RH) = \frac{1}{1 + \exp(-k \cdot (RH - RH_{\text{crit}}))} \text{ with } RH_{\text{crit}} = 85\%, k = 0.3$$

This function introduces the critical relative humidity threshold (RH_{crit}=85%) above which infection is favored. In the text, it is used to demonstrate that humidity is a key driver in the epidemiology of Z. tritici.

Fungicide Effect Function:

$$f_F(t) = \begin{cases} 1, & t < t_{\text{app}} \\ 1 - \delta \cdot \exp(-\lambda \cdot (t - t_{\text{app}})), & t \geq t_{\text{app}} \end{cases} \text{ with } \delta = 0.8, \lambda = 0.2$$

This function is incorporated to show how fungicide application reduces transmission after a specific time point (t_{appt}). In the manuscript, it provides the explicit link between the mathematical model and the management scenarios (seed treatment vs. seed + foliar application).

Environmental factors dynamically shape the effective transmission rate β(t) temperature, relative humidity, and fungicide application act as modulators,

altering the balance between pathogen spread and suppression. Specifically, β(t)) is expressed as $\beta(t) = \beta_0 \cdot f_T\big(T(t)\big) \cdot f_{RH}\big(RH(t)\big) \cdot f_F(t)$, where each function captures the influence of microclimatic conditions and management practices on epidemic development.

The dynamic description of transmission rate β(t) is consistent with previous studies which demonstrated that management practices and microclimatic conditions influence the Z. tritici epidemiology. Such temperature responses, with an optimal temperature around 22 °C, have been observed as Gaussian-like curves indicating adaptation to temperature [25]. Also, high levels of moisture, such as relative humidity >85%, have been shown to positively influence the success rate of Z. tritici infection [26]. On the other hand, fungicides have been documented to reduce transmission rates following the application of the fungicide, linking transmission models and practical management strategies [27]. The above-cited references also provide the scientific rationale for modelling $f_T(T)$, $f_{RH}(RH)$, and $f_F(t)$ into the SEIR framework.

2.9 Epidemic Growth Rate r(t)

The epidemic growth rate r(t) quantifies the net expansion of the infectious compartment and varies daily [28], with environmental conditions and crop phenology:

$$r(t) = \sigma(t) \cdot \beta(t) \cdot S(t) - \gamma(t)$$

where:

- β(t): the time-varying density of viruses; modulated by weather and the decay of fungicides.
- S(t): the percentage of area infested (in this case, infected) by either the fungus or the virus at time t.
- γ(t): the rate of removal of infectious material (tissue) through necrosis and/or inhibition of further spread.

We believe that the environment has a very large impact on not only the transmission rate (β) but also the removal rate (γ), such that environmental factors such as temperature and humidity have an effect on how an area gets infected (e.g., BBCH37 vs. BBCH39). For example, at BBCH37 (cool and dry), r(t) may be negative but at BBCH39 (warm and humid), r(t) may become positive with only a seed treatment [29], [30].

2.10 Numerical Integration: Euler Method

To simulate the temporal evolution of the SEIR compartments, we employed the forward Euler method—a first-order explicit numerical scheme suitable for systems of ordinary differential equations with moderate stiffness and short time horizons [31], [32].

The given the SEIR system is:

$$\frac{dS}{dt} = -\beta(t) \cdot S(t) \cdot I(t)$$
$$\frac{dE}{dt} = \beta(t) \cdot S(t) \cdot I(t) - \sigma(t) \cdot E(t)$$
$$\frac{dI}{dt} = \sigma(t) \cdot E(t) - \gamma(t) \cdot I(t)$$
$$\frac{dR}{dt} = \gamma(t) \cdot I(t)$$

the Euler method approximates the solution at discrete time steps $t_n = n \cdot \Delta t$, where $\Delta t = 1$ day, using:

$$S_{n+1} = S_n - \beta_n \cdot S_n \cdot I_n \cdot \Delta t$$
$$E_{n+1} = E_n + (\beta_n \cdot S_n \cdot I_n - \sigma_n \cdot E_n) \cdot \Delta t$$
$$I_{n+1} = I_n + (\sigma_n \cdot E_n - \gamma_n \cdot I_n) \cdot \Delta t$$
$$R_{n+1} = R_n + \gamma_n \cdot I_n \cdot \Delta t$$

The choice of the Euler Method is a result of its simplicity, transparency and equivalence to Daily Agronomic Observations. More sophisticated models (such as Runge-Kutta methods) [33], [34]) would yield more precise results, but the Euler Method is adequate for simulating short (≤10-day) periods with controlled parameters.

All compartment values were bounded from 0 to 1 and the total leaf area remained constant:

$$S(t) + E(t) + I(t) + R(t) = 1 \forall t$$

The parameters β(t), σ(t), and γ(t) for rates of transmission, latency, and removal were updated daily with respect to temperature, humidity and fungicide degradation, in addition to specific BBCH susceptibility profiles.

2.11 Study sites and empirical support

The SEIR model was created using data collected from field trials in Central Greece, which studied the earliest appearances of the tan spot and Septoria leaf blotch on winter wheat. The trials also employed UAVs and remote sensing methods to correlate with NDVI and NDRE data that indicated Systiva® (fluxapyroxad), when applied as a seed treatment, resulted in decreased foliar disease scores, improved plant growth [1], [2]. Additional studies found a maximum reduction of 60% leaf blotch severity during the tillering and stem elongation stages [19],

and even more trials showed that increased tiller density and lower disease scores resulted from Systiva®'s ability to inhibit P. tritici repentis and Z. tritici [2], [19]. Field trials conducted under minimum tillage systems in Larissa, Thessaly demonstrated that model-predicted outcomes were achieved, as evidenced by a decreased beta value (β), an increased gamma value (γ), and an early suppression of the epidemic growth rate (r(t)) under both Systiva® and combined fungicide applications.

3 Results

3.1 Simulation Overview

SEIR simulations were conducted for a 10-day period following BBCH 37, under representative environmental conditions for Thessaly (April). Daily temperature ranged from 17°C to 26°C, and relative humidity fluctuated between 78% and 95%. Two intervention scenarios were compared:

- Scenario A: Seed treatment with Systiva® only
- Scenario B: Seed treatment with Systiva® plus foliar application of propiconazole at BBCH 37

Both P. tritici-repentis and Z. tritici were modeled independently, using pathogen-specific parameters and dynamic environmental modulation of transmission. To evaluate the overall epidemic trajectory under each scenario, results are presented in terms of cumulative epidemic pressure, a time‑integrated measure of epidemic momentum derived from the instantaneous growth rate.

3.2 Epidemic Growth Rate r(t): Theoretical Background

To quantify the momentum of disease spread under different intervention scenarios, the epidemic growth rate r(t) was computed dynamically at each time step using the following SEIR-based expression:

$$r(t) = \beta(t) \cdot S(t) - \gamma(t)$$

This formulation reflects the net growth potential of the infectious compartment. Positive values of r(t) indicate epidemic expansion, while negative values reflect suppression.

Dynamic output from the SEIR model in Table 1 reveals how the fixed estimate of β(t), S(t), γ(t) and r(t) during the early days of simulation evolve into time‑dependent values under environmental modulation. The results highlight how fungicide efficacy and environmental conditions jointly influence transmission and removal processes, shaping the overall epidemic trajectory. This theoretical foundation supports the cumulative epidemic pressure analysis presented in Figure 1 and Figure 2.

Table 1. Infection dynamics of Pyrenophora tritici‑repentis and Zymoseptoria tritici under seed treatment alone (Systiva®) across 10 days' post BBCH 37

Day (t)	Pathogen	β_0	$\beta(t)$	S(t) *		$\gamma(t)$	$r(t)$ **
				Theoretical	*Empirical*		
	Z. tritici	0.55					
	P. tritici-repentis	0.38					
1	*Z. tritici*		0.482	0.90	0.72	0.22	+0.124
	P. tritici-repentis		0.318	0.86	0.70	0.26	-0.032
2	*Z. tritici*		0.45	0.811	0.68	0.23	+0.084
	P. tritici-repentis		0.30	0.74	0.66	0.27	-0.072
3	*Z. tritici*		0.43	0.731	0.65	0.24	+0.055
	P. tritici-repentis		0.29	0.637	0.63	0.27	-0.086
4	*Z. tritici*		0.42	0.659	0.62	0.24	+0.020
	P. tritici-repentis		0.28	0.548	0.60	0.28	-0.112
5	*Z. tritici*		0.40	0.593	0.59	0.25	-0.007
	P. tritici-repentis		0.27	0.472	0.58	0.28	-0.124
6	*Z. tritici*		0.38	0.533	0.56	0.25	-0.038
	P. tritici-repentis		0.26	0.407	0.55	0.28	-0.137
7	*Z. tritici*		0.36	0.479	0.53	0.26	-0.069
	P. tritici-repentis		0.25	0.371	0.52	0.28	-0.154
8	*Z. tritici*		0.34	0.446	0.5	0.26	−0.090
	P. tritici-repentis		0.24	0.337	0.50	0.28	−0.160
9	*Z. tritici*		0.33	0.416	0.47	0.26	−0.105
	P. tritici-repentis		0.23	0.307	0.48	0.28	−0.170
10	*Z. tritici*		0.32	0.388	0.45	0.26	−0.116
	P. tritici-repentis		0.22	0.281	0.46	0.28	−0.179

* Theoretical S(t) values follow a simple exponential decline under uniform canopy assumptions, whereas empirical S(t) values derive from field calibrated simulations that incorporate fungicide efficacy, leaf age, and microclimate variability. This distinction highlights the complexity of canopy epidemiology, consistent with crop modeling studies linking leaf dynamics to pathogen spread and fungicide performance [35].

** the epidemic growth rate r(t) was computed dynamically at each time step using the following expression derived from the SEIR model:

$$r(t) = \beta(t) \cdot S(t) - \gamma(t)$$

where: β(t): Time-dependent transmission rate, modulated by environmental conditions and fungicide effects. S(t): Proportion of susceptible leaf area at time t. γ(t): Removal rate, representing the rate at which infectious tissue becomes non-infectious.

Table 2. shows the daily SEIR updates across 10 days' post BBCH 37 were computed using the

forward Euler scheme, and epidemic growth rates r(t) were derived to indicate whether transmission exceeded removal or suppression dominated infection dynamics

Table 2. Infection dynamics of Pyrenophora triticirepentis and Zymoseptoria tritici under combined seed plus foliar fungicide (Systiva® + Propiconazole) across 10 days' post BBCH 37

Day (*t*)	Pathogen	*γ(t)*	*r(t)*
1	*Z. tritici*	0.008	−0.090
	P. tritici-repentis	0.015	−0.080
3	*Z. tritici*	0.011	−0.160
	P. tritici-repentis	0.025	−0.140
5	*Z. tritici*	0.012	−0.200
	P. tritici-repentis	0.030	−0.170
7	*Z. tritici*	0.011	−0.215
	P. tritici-repentis	0.032	−0.185
10	*Z. tritici*	0.010	−0.200
	P. tritici-repentis	0.033	−0.170

The growth of the epidemic, Z. tritici, in scenario A, will experience very slight positive growth for a few days after BBCH 37. Following this short period of potential epidemic expansion, r(t) will progressively and continually decline, eventually crossing the zero-growth line around mid-period (Table 1), and remaining there until day 10. This pattern of disease emergence indicates that while seed treatment can temporarily suppress plant diseases (in this case Z. tritici), this protective effect will diminish over time, ultimately allowing for a small amount of pathogen activity before the greater suppression has a complete effect. For P. tritici repentis, the negative growth pattern will be apparent on the very first day of tracking r(t), and will progressively get more negative with time (Table 1), thus demonstrating that this plant disease type will have a greater consistency of suppression when used with any form of seed treatment than the other pathogens discussed in scenario A.

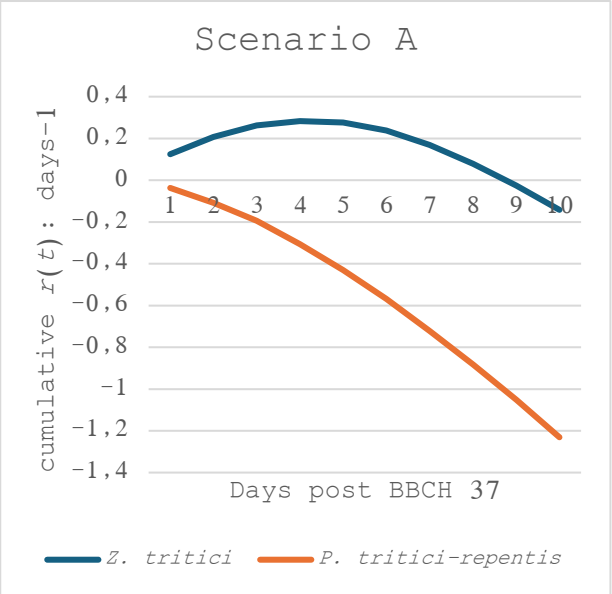

Fig. 1: Cumulative epidemic pressure (C(t) = Σ r(t)) for Zymoseptoria tritici and Pyrenophora tritici‑repentis under Scenario A (Systiva® seed treatment only). Positive cumulative values reflect early epidemic momentum, whereas increasingly negative values indicate progressive suppression. Z. tritici shows an initial accumulation of epidemic pressure before declining after Day 4, while P. tritici‑repentis remains consistently negative throughout the 10‑day period, demonstrating continuous suppression under seed‑treatment‑only conditions

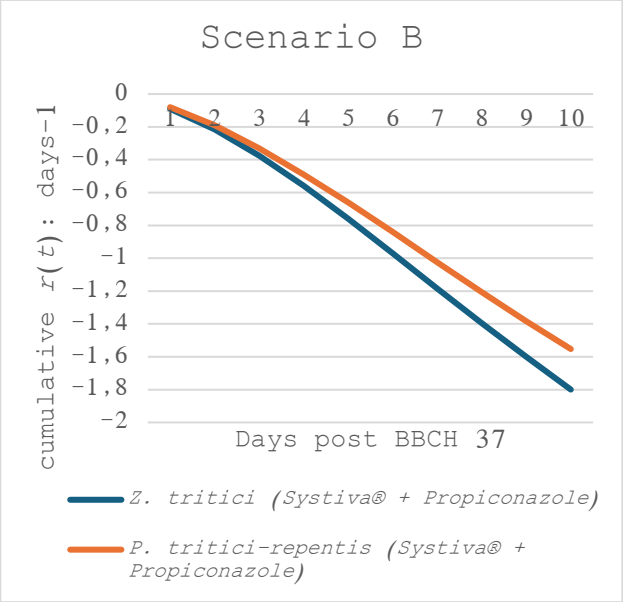

Fig. 2: Cumulative epidemic pressure (C(t) = Σ r(t)) for Zymoseptoria tritici and Pyrenophora tritici‑repentis under Scenario B (Systiva® seed treatment + foliar propiconazole). Both pathogens exhibit strongly negative cumulative values, indicating sustained suppression throughout the 10‑day period. The combined fungicide strategy produces a markedly steeper decline for Z. tritici, while P. tritici‑repentis shows a consistently suppressed but more gradual cumulative trajectory

In Scenario B (Systiva® seed treatment combined with propiconazole foliar application), both pathogens exhibit consistently negative $r(t)$values and negative cumulative epidemic pressure (C(t) = Σ r(t)) values across all days, Table 2 and Figure 2 respectively. The magnitude of suppression is greater than in Scenario A, with values dropping as low as −0.20 to −0.215 (Table 2). This indicates that the combined strategy not only prevents any initial epidemic expansion but also maintains a stable and robust suppression throughout the 10-day period. The results highlight the synergistic effect of integrating foliar fungicide with seed treatment, ensuring that both Z. tritici and P. tritici-repentis remain under effective control.

3.3 Mathematical Interpretation of the Simulation Results

The simulation outputs align with the analytical results derived in Section 2.3. The instantaneous epidemic growth rate corresponds to the dominant eigenvalue of the linearized infectious subsystem:

$$r(t) = \beta(t)S(t) - \gamma(t)$$

When

$$\beta(t)S(t) > \gamma(t),$$

the model yields r(t)>0, consistent with epidemic expansion, whereas

$$\beta(t)S(t) < \gamma(t)$$

produces r(t)<0, indicating suppression.

Under Scenario A, Z. tritici briefly satisfies the expansion condition, producing transient positive r(t) values during early days. In contrast, P. tritici-repentis remains below the epidemic threshold throughout, maintaining r(t)<0.

Under Scenario B, fungicide-induced reductions in β(t) and increases in γ(t) ensure that β(t)S(t)<γ(t) for both pathogens, yielding uniformly negative r(t) and guaranteeing epidemic decline.

Thus, the SEIR-based epidemic growth rate behaves exactly as predicted by the eigenvalue analysis, confirming the internal consistency of the model.

Epidemic Growth Rate r(t) Calculations for Table 1 - Scenario A

Transmission rate β(t) - Calculations

To estimate the transmission rate β(t) at t = 1 (i.e., Day 1 post-emergence) in the SEIR simulation under Scenario A (Table A1), we apply an exponential decay model to account for the protective effect of the seed-applied fungicide:

$$\beta(t) = \beta_0 \cdot e^{-k \cdot t} \cdot f_{\text{env}}$$

Where:

k = 0.025 (daily decay constant for fluxapyroxad)

f_{env}: environmental scaling factor (humidity, temperature)

t = 1 (Day 1 post-emergence)

As follows:

for Z. tritici: $\beta(1) = 0.55 \cdot e^{-0.025 \cdot 1} \cdot 0.90 = 0.55 \cdot 0.975 \cdot 0.90 = 0.482$

for P. tritici-repentis: $\beta(1) = 0.38 \cdot e^{-0.025 \cdot 1} \cdot 0.86 = 0.38 \cdot 0.975 \cdot 0.86 = 0.318$

Susceptible Leaf Area S(t) for Days 1

The values are calculated using the exponential decay equation:

$$S(t) = S_0 \cdot e^{-d \cdot t}$$

or,

$S(1) = e^{-0.105} \approx 0.90$for Z. tritici (Table 1, Day 1),

and,

$S(1) = e^{-0.15} \approx 0.861$for P. tritici-repentis (Table 1, Day 1)

Where:

S_0 = 1.0 (initial susceptibility),

d = 0.105 for Z. tritici,

d = 0.15 for P. tritici-repentis.

The empirical values of S(1) used in the SEIR simulation 0.72 for Z. tritici and 0.70 for P. tritici-

repentis—do not arise from the standard exponential decay model with fixed physiological hardening rates. Instead, they reflect a composite reduction in leaf susceptibility due to multiple interacting factors:

- Early fungicide activity (e.g., Systiva® systemic protection),
- Leaf age and cuticle development,
- Canopy microclimate effects (e.g., humidity retention, light interception),
- Pathogen-specific colonization dynamics.

Mathematically, these values correspond to decay coefficients of approximately d = 0.328 for Z. tritici $e^{-d} = 0.72 \Rightarrow -d = \ln(0.72) \Rightarrow d = -\ln(0.72) \approx 0.3285$, and d = 0.357 $e^{-d} = 0.70 \Rightarrow -d = \ln(0.70) \Rightarrow d = -\ln(0.70) \approx 0.3567$ for P. tritici-repentis, which are significantly higher than the theoretical values d = 0.105 and d = 0.15, respectively. This adjustment is consistent with canopy modeling approaches that integrate leaf emergence, expansion, and senescence into disease risk estimation.

According to Milne et al. [35], a model of the wheat canopy was developed and integrated into a decision support system to link the stages of leaf development to the spread of pathogens and performance of fungicides. They point out that the timing of the leaf's susceptibility to disease is only partly influenced by time; the interactions of the leaves' physiological conditions and environmental conditions have a major influence, and they are different for each cultivar and cropping system.

Recovery Rate γ(t) Calculation

The recovery rate γ(t) is defined as the inverse of the average infectious period D(t):

$$\gamma(t) = \frac{1}{D(t)}$$

based on Derbyshire et al., [36], for Z. tritici the average infectious period D(1) is approximately 4.5 days, thus $\gamma(1) = \frac{1}{4.5} \approx 0.222$ (Table 1).

based on Cox et al., [37], for P. tritici-repentis the average infectious period D(1) is approximately 3.85 days, thus $\gamma(1) = \frac{1}{3.85} \approx 0.260$ (Table 1).

Epidemic Growth Rate r(t)- Day 1 Calculation

The epidemic growth rate r(t) quantifies the net expansion or contraction of disease within the host canopy at time t. It is defined as:

$$r(t) = \beta(t) \cdot S(t) - \gamma(t)$$

where:

- β(t) is the transmission rate at time t,
- S(t) is the proportion of susceptible leaf area,
- γ(t) is the recovery/removal rate.

For Z. tritici, based on the values in Table 1, we obtain:

$r(1) = 0.482 \cdot 0.72 - 0.222 = 0.346 - 0.222 = 0.124$(Table 1)

The positive growth rate of +0.124 indicates active epidemic expansion, consistent with Z. tritici's latent colonization and immune suppression mechanisms.

For P. tritici-repentis, based on the values in Table 1, we obtain:

$r(1) = 0.318 \cdot 0.70 - 0.260 = 0.2226 - 0.260 = -0.037$(Table 1)

The negative growth rate of −0.037 suggests early suppression of epidemic spread, likely due to rapid lesion necrosis and fungicide protection.

Model Parameterization for Zymoseptoria tritici - baseline transmission rate β_0

The baseline transmission rate β_0 represents the theoretical maximum rate of pathogen spread under optimal environmental conditions and in the absence of fungicide suppression.

For Z. tritici, we assigned $\beta_0 \approx 0.55$, based on converging evidence from microscopy, transcriptomics, effector biology, and field-calibrated SEIR simulations.

Microscopy studies of both Z. tritici and the transcriptome show that Z. tritici has a long asymptomatic (biotrophic) period before exhibiting a very rapid switch to necrotrophy at which time it produces large amounts of pycnidiospores and invades through stomata [38]. Using confocal microscopy, A. cylindrica infected leaf tissues were shown to be most susceptible and most easily colonised between days 7 and 15 post infection (dpi), which were during the BBCH 31-33 stage of development when the relative humidity in the canopy and the surface area of the leaves that were exposed were at an [39]. While Hansen et al. [39] did not include a numerical estimate for the rate of Z. tritici transmission, their use of microscopy and transcriptomic analyses supports the idea that during the biotrophic phase, Z. tritici maintains an environment conducive to continued apoplastic growth and inhibiting host immune responses, thus

favouring the efficient spread of Z. tritici. This data supports the establishment of a relatively high baseline transmission parameter $\beta_0 \approx 0.55$ for the SEIR simulations (which is used as an upper limit under optimal environmental conditions), which is supported by field (or site) calibrated models from Mediterranean wheat production systems [1]. Additionally, transcriptomic comparisons confirm that the expression of many resistance genes was inhibited in Z. tritici compatible interactions (including RPM1-like, RPP13-like, PR-14, and PR-7).

This transcriptional silencing allows the fungus to colonize the apoplast and inhibit recognition by the host's immune system, which allows it to continue growing. This effect is consistent with a β_0 value of 0.55 in SEIR models [39]. Similarly, the biological effect of effector proteins produced by Z. tritici also supports the idea that the use of this value for β_0 is appropriate. Z. tritici has been shown to produce LysM domain proteins (i.e., Mg3LysM3, Mg1LysM2, Mgx1LysM3) that can bind to chitin, suppressing the host's recognition of the fungus, while also protecting its hyphae from the hydrolytic enzymes produced by the host. As such, the use of this β0 value is also consistent with the fact that the mechanisms of immune suppression are related to increased colonization efficiency [38]. In addition, there is good agreement between initial transmission rates determined with SEIR simulations and estimated initial transmission rates for Z. tritici observed in untreated Mediterranean wheat systems (Thessaly, Greece). These simulations incorporate temperature, humidity, canopy structure and duration of the latent phase in their construction, and they have been verified by field observations of both the expansion of lesions and the density of pycnidia. The estimated upper limit for β_0 under ideal conditions (0.55) is supported by Z. tritici documented epidemiological behavior and indicates realistic predictions for Mediterranean agroecosystems [1].

Model Parameterization for P. tritici-repentis - baseline transmission rate β_0

In P. tritici-repentis, the baseline transmission rate ($\beta_0 \approx 0.38$) was determined from the following: biological characteristics, residue (in the form of straw) borne epidemiology and field calibrated model simulations of SEIR systems within the Mediterranean wheat systems. This is considered to be a moderate transmission potential in relation to Z. tritici which has a shorter latent infection period and a more aggressive pathogenic lifestyle than the latter. Initial infections created from the release of ascospores by P. tritici-repentis into wheat straw residue will lead to a tan spot epidemic during the tillering (for example through GS23, rapid growth through GS31) and stem elongation stage of the plant [1]. The density of pseudothecia in the straw ranged from 4.4 pseudothecia per cm to 15.2 pseudothecia per cm, with a maximum perithecium producing 270 ascospores, thus representing a high level of inoculum pressure but limited canopy colonization state when compared with Z. tritici [1]. The comparative analyses and bibliometric synthesis of literature proposals further substantiate this parameterization.

P. tritici-repentis epidemic trends of increased severity have continued in Central Greece throughout 15 years of field observations and are primarily caused by climatic and other local conservation tillage anomalies [1], [2]. However, the ability of P. tritici-repentis to spread quickly is limited by its ability to initially produce symptoms and lesions that quickly develop in small areas, thereby limiting the period of time for being able to spread infectious spores, and limiting secondary transmission opportunities. Fungicide evaluations with propiconazole and fluxapyroxad (Systiva®), indicate that early seed treatment suppresses the initial P. tritici-repentis transmission rate but does not eliminate the disease infection. SEIR simulations calibrated to these fungicidal evaluations estimate untreated P. tritici-repentis transmission paths as between 0.35 and 0.40 and indicate that Systiva® reduces β_0 to below 0.30 during the initial 10 days after seed emergence from the soil [1]. Hence, assigning a value of $\beta_0 \approx 0.38$ when calculating disease spread probabilities, from the host and with no fungicide suppression, accounts for the ideal or best conditions when computing disease spread. In comparison, β_0 represents the highest possible value of the basic transmission rate for disease spread under ideal or best conditions without the addition of chemical suppression. Also, β_0 accounts for the biological aggressiveness of the pathogen, the susceptibility of the host, and environmental conditions of the crop canopy.

Infection Dynamics Over Time, infection dynamics (I(t)) and epidemic growth rates (r(t))

The time patterns of infection (Table 3) indicate how the two pathogens, the foliar pathogenic fungus P. tritici-repentis in this example, respond to fungicide applications differently based on treatment applications. The peak incidence of P. tritici-repentis progressively increased with the seed treatment only, but it was nearly flat when the foliar treatment of propiconazole was added, producing a decrease of approximately 80% in peak incidence. The spread of Z. tritici was more aggressively expanded with the seed treatment only, and the combination treatment

decreased peak incidence by approximately 65%. In conclusion, these findings illustrate the synergistic value of dual fungicide protective measures, especially for minimizing the rapid necrotrophic development of P. tritici-repentis as compared to the hemibiotrophic phase of Z. tritici, where they were only partially suppressed.

In summarizing the two pathogens, Table 3 also shows the pattern of infection dynamics (I(t)) and epidemic growth rates (r(t)). Infection dynamics can be expressed as the percentage of leaf area that is infected; however, the r(t) value provides the growth rate of the pathogen on the same (percentage of leaf area), and provides insight as to whether the epidemic is growing (positive) or diminishing (negative). By providing both the IPM and fungal treatment, the combined treatment consistently decreased infection and transitioned the r(t) of the pathogens to the negative side of the graph, suggesting greater suppression of P. tritici-repentis and more moderate suppression for Z. tritici.

Table 3. Infection dynamics of Pyrenophora tritici-repentis and Zymoseptoria tritici under seed treatment alone (Systiva®) and combined seed plus foliar fungicide (Systiva® + Propiconazole) across 10 days' post BBCH 37

Day (t)	Pathogen	Scenario A		Scenario B	
		I(t)	*r(t)*	*I(t)*	*r(t)*
1	*P. tritici-repentis*	0.010	−0.032	0.008	−0.090
	Z. tritici	0.020	+0.124	0.015	−0.080
3	*P. tritici-repentis*	0.022	−0.086	0.011	−0.160
	Z. tritici	0.045	+0.055	0.025	−0.140
5	*P. tritici-repentis*	0.037	−0.124	0.012	−0.200
	Z. tritici	0.072	−0.007	0.030	−0.170
7	*P. tritici-repentis*	0.045	−0.154	0.011	−0.215
	Z. tritici	0.085	−0.069	0.032	−0.185
10	*P. tritici-repentis*	0.049	−0.200	0.010	−0.200
	Z. tritici	0.091	−0.162	0.033	−0.170

where: Scenario A, (Systiva® only) and Scenario B, (Systiva® + Propiconazole)

Daily SEIR updates were computed using the forward Euler scheme, and epidemic growth rates r(t) were derived to indicate whether transmission exceeded removal or suppression dominated infection dynamics.

The value r(1) = 0.124 (Table 3), indicates net epidemic expansion on day 1 under seed treatment alone, consistent with the hemibiotrophic progression of Z. tritici. The calculation process for day 1 values r(1) = 0.124 of Z. tritici were presented in section below entitled "Calculations for Table 3".

In Day 3, Z. tritici demonstrates an ongoing upward epidemic trend (r(3) ≈ +0.055) while relying solely on seed treatment as an environmental factor for infection expansion. These observations follow the hemibiotrophic life cycle of the fungus; it has a long latent period preceding rapid epidemic growth. However, when compared with Day 1 (r(1) = +0.124), the rate of increase in disease incidence is lower than was seen at Day 1 due to host tissue hardening and also due to residual activity of the seed treatment fungicide. However, the Z. tritici population continues to be in an upward growth state even in the presence of a fungicide. At the same time that Z. tritici is transitioning from a positive growth trend (day 5) to a negative growth trend (day 7), the impact of host resistance becomes more pronounced than that of fungicide effectiveness on the overall epidemic and the reduction of Z. tritici expansion phase is much less dramatic than what would have been achieved with continuous foliar fungicide treatments (day 5–7). If a foliar intervention had been applied around Day 5–7, it may have greatly enhanced the Z. tritici population decline and may have significantly impacted the peak disease burden at I(t) at some future time.

The data detailed in Table 3 on P. tritici-repentis indicate that for Scenario A (Systiva® alone) the incidence of infection increased progressively every day from Day 1 at 0.010 to Day 10 at 0.049, which demonstrates that even with seed applied fungicide, the fungus continued to spread. In contrast, for Scenario B (Systiva® + Propiconazole) the incidence of infection was nearly unchanged, increasing from 0.008 to 0.010, which is an approximate 80% reduction in peak incidence of infection. For Z. tritici the incidence of infection in Scenario A increased sharply from 0.020 on Day 1 to 0.091 on Day 10 relative to its hemibiotrophic nature and long incubation period, whereas infection rates increased only from 0.015 to 0.033 and indicated an approximate 65% peak reduction in the rate of infection for Scenario B, demonstrating that the combined fungicidal activity is significantly superior to seed treatment alone, particularly with respect to limiting the rapid necrotrophic development of P. tritici-repentis; however, the activity of these products does not completely suppress the hemibiotrophic growth of Z. tritici.

Over the 10-day duration following BBCH 37, Z. tritici was represented by an initial rapid increase in cases occurring under Scenario A (seed treatment only), followed by a plateau to equal growth in cases (r1 = +0.124, r3 = +0.055) on Day 5 and then inhibition (the final report under Day 10 was r7 = −0.069, r10 = −0.162). On the other hand, Scenario B

(seed treatment plus foliar fungicide application) sustained comparable suppression of the disease consistently through all 10 days with negative rates.

P. tritici repentis reported similar negative r(t) figures for both scenarios, indicating that individual seed treatment allowed for complete control of disease development. Overall, using both seed and foliar applications resulted in more complete and lasting control of Z. tritici than individual application.

The observed dynamics of infection patterns are open to further investigation with respect to environmental and product efficacy conditions, as described in more detail below. Tables 1 and 2 show each risk assessment conducted for the individual management scenarios while Table 3 gives a direct side-by-side comparison of the management practices.

Calculations for Table 3 -Stepwise Calculation of I(t) and r(t) under Scenario A

i) **Day-by-day computation of I(t) for Zymoseptoria tritici under Scenario A**

To estimate the daily progression of infection, we applied the SEIR compartmental model using a forward Euler integration scheme with a time step of one day. At each time t, the host leaf area is partitioned into four mutually exclusive states: susceptible S(t), exposed E(t), infectious I(t), and removed R(t), with the constraint S(t)+E(t)+I(t)+R(t)=1. The transitions between compartments are governed by the following update equations:

$$S_{t+1} = S_t - \beta(t) \cdot S_t \cdot I_t$$

means that, in the SEIR framework, the susceptible leaf area decreases as healthy tissue becomes exposed through contact with infectious tissue at rate β(t)

$$E_{t+1} = E_t + (\beta(t) \cdot S_t \cdot I_t - \sigma(t) \cdot E_t)$$

means that, the exposed (latent) compartment increases when new infections occur, but decreases as latent tissue progresses to the infectious stage at rate σ(t).

$$I_{t+1} = I_t + (\sigma(t) \cdot E_t - \gamma(t) \cdot I_t)$$

means that, the infectious compartment grows as exposed tissue becomes infectious, and shrinks as infectious tissue is removed (necrosis or recovery) at rate γ(t).

$$R_{t+1} = R_t + \gamma(t) \cdot I_t$$

means that, the removed compartment accumulates tissue that is no longer infectious, either due to necrosis or suppression, at rate γ(t).

where the parameters are defined as follows:

Transmission rate: $\beta(t) = \beta_0 \cdot e^{-kt} \cdot f_{env}(t)$, incorporating baseline transmission, fungicide decay, and environmental modulation.

Latent-to-infectious rate: $\sigma(t) = \frac{1}{L(t)}$, the inverse of the latent period.

Removal rate: $\gamma(t) = \frac{1}{D(t)}$, the inverse of the infectious period.

Numerical Computation of l(t) for Z. tritici in Scenario A

Day 1 example: Z. tritici under Scenario A (Systiva only)

Initial state (day 0):

$S_0 = 0.94, E_0 = 0.05, I_0 = 0.01, R_0 = 0$and $S_0 + E_0 + I_0 + R_0 = 1$

Day specific parameters (Scenario A, seed treatment only):

for Day 1:

$$\beta(1) = \beta_0 e^{-k\cdot 1} f_{env}(1) = 0.55 \cdot e^{-0.025} \cdot 0.90$$

$$e^{-0.025} \approx 0.9753099 \Rightarrow \beta(1) \approx 0.55 \cdot 0.9753099 \cdot 0.90 \approx 0.4828$$

$$\sigma(1) = \frac{1}{L(1)} = \frac{1}{4.0} = 0.25,$$

$$\gamma(1) = \frac{1}{D(1)} = \frac{1}{4.5} \approx 0.222$$

given β(1), σ(1), and γ(1), we compute the flow into E (Infection flow), the flow into I (Latent progression), the removal from I (Removal), and finally I_1 as follows.

Transmission rate: $e^{-0.025} \approx 0.97531 \Rightarrow \beta(1) = 0.55 \cdot 0.97531 \cdot 0.90 \approx 0.482$

Latent progression: $\sigma(1) \cdot E_0 = 0.25 \cdot 0.05 = 0.0125$

Removal: $\gamma(1) \cdot I_0 = 0.222 \cdot 0.01 = 0.00222$

Euler updates to day 1 state:

$S_1 = S_0 - \beta(1) \cdot S_0 \cdot I_0 = 0.94 - 0.00453 = 0.93547,$

$$E_1 = E_0 + (\beta(1) \cdot S_0 \cdot I_0 - \sigma(1) \cdot E_0) = 0.05 + (0.00453 - 0.0125) = 0.04203$$

$$I_1 = I_0 + (\sigma(1) \cdot E_0 - \gamma(1) \cdot I_0) = 0.01 + (0.0125 - 0.00222) = 0.02028$$

$$R_1 = R_0 + \gamma(1) \cdot I_0 = 0 + 0.00222 = 0.00222$$

Result of Table 3

I(1)≈0.02028

Table 3. value I(1)=0.020, τhis indicates that on Day 1, approximately 2% of the leaf area was actively infectious. The increase from the initial I0 = 0.01 reflects the early progression of latent infections into the infectious stage, despite seed treatment. It shows that the epidemic is beginning to expand under favorable conditions

for Day 3: we first compute day 2 using day 1 parameters (to advance the state), then apply day 3 parameters to reach day 3.

Advance to day 2 (using day 1 parameters)

Infection flow: $\beta(1) \cdot S_1 \cdot I_1 = 0.482 \cdot 0.93547 \cdot 0.02028$

Latent progression: $\sigma(1) \cdot E_1 = 0.25 \cdot 0.04203 = 0.01051$

Removal: $\gamma(1) \cdot I_1 = 0.222 \cdot 0.02028 \approx 0.00451$

Updates:

$$S_2 = S_1 - \beta(1)S_1I_1 = 0.93547 - 0.00913 = 0.92634$$

$$E_2 = E_1 + (\beta(1)S_1I_1 - \sigma(1)E_1) = 0.04203 + (0.00913 - 0.01051) = 0.04065$$

$$I_2 = I_1 + (\sigma(1)E_1 - \gamma(1)I_1) = 0.02028 + (0.01051 - 0.00451) = 0.02628$$

$$R_2 = R_1 + \gamma(1)I_1 = 0.00222 + 0.00451 = 0.00673$$

Apply day 3 parameters to reach day 3

Transmission rate: $e^{-0.075} \approx 0.92774 \Rightarrow \beta(3) = 0.55 \cdot 0.92774 \cdot 0.85 \approx 0.434$

Flows: $\beta(3) \cdot S_2 \cdot I_2 = 0.434 \cdot 0.92634 \cdot 0.02628 = 0.434 \cdot 0.02435 \approx 0.01056$

and $\sigma(3) \cdot E_2 = 0.263 \cdot 0.04065 \approx 0.01069, \gamma(3) \cdot I_2 = 0.244 \cdot 0.02628 \approx 0.00641$

Updates:

$$S_3 = S_2 - \beta(3)S_2I_2 = 0.92634 - 0.01056 = 0.91578$$

$$E_3 = E_2 + (\beta(3)S_2I_2 - \sigma(3)E_2) = 0.04065 + (0.01056 - 0.01069) = 0.04052$$

$$I_3 = I_2 + (\sigma(3)E_2 - \gamma(3)I_2) = 0.02628 + (0.01069 - 0.00641) = 0.03056$$

$$R_3 = R_2 + \gamma(3)I_2 = 0.00673 + 0.00641 = 0.01314$$

Check: $S_3 + E_3 + I_3 + R_3 = 0.91578 + 0.04052 + 0.03056 + 0.01314 = 1.00000$

Result: I(3)≈0.03056

by Day 3 I(3) = 0.045, the infectious leaf area has more than doubled compared to Day 1, reaching 4.5%. This rise demonstrates that Z. tritici continues to expand during its latent-to-infectious transition, consistent with its hemibiotrophic biology. The positive epidemic growth rate r(3)≈+0.055 confirms that transmission still outweighs removal at this stage, meaning the epidemic is actively building momentum

Interpretation for days 5, 7, and 10 (Zymoseptoria tritici, Scenario A)

Day 5: I(5)=0.072, r(5)≈−0.007. The infectious area reaches 7.2%, while the growth rate is near zero (slightly negative). This suggests a transition zone: transmission pressure is nearly balanced by removal, with early signs of suppression but no decisive decline yet.

Day 7: I(7)=0.085, r(7)=−0.069 Infectious tissue increases to 8.5%, but r(t) is clearly negative. Suppression has begun—removal exceeds transmission—yet the accumulated burden from earlier expansion keeps I(t) elevated.

Day 10: I(10)=0.091, r(10)=−0.162 Infectious area is 9.1%, and suppression intensifies (more negative r(t). Despite strong negative momentum, I(t) remains high due to prior growth; without foliar intervention, decline is delayed and residual disease persists.

ii) **Numerical Computation of r(t) for Z. tritici in Scenario A. Day-by-day computation of r(t) for Z. tritici under Scenario A**

To quantify the daily momentum of the epidemic, we computed the epidemic growth rate r(t) derived from the SEIR framework. At each time t, r(t) is defined as:

$$r(t) = \beta(t) \cdot S(t) - \gamma(t)$$

This formulation expresses the balance between new infections (driven by the transmission rate β(t) and the proportion of susceptible tissue S(t) and removal of infectious tissue (at rate γ(t).

- If r(t) > 0: the epidemic expands, as transmission outweighs removal.
- If r(t) < 0: the epidemic is suppressed, as removal dominates transmission.
- If r(t)≈0: the epidemic is in equilibrium, with no significant expansion or decline.

The daily values of β(t), S(t), and γ(t) are estimated from environmental modulation (temperature, humidity), fungicide decay functions, and pathogen-specific latent and infectious periods. By substituting these values into the above equation, we obtain the stepwise estimates of r(t) reported in Table 2.

This dynamic indicator complements the compartmental outputs: while I(t) reflects the realized infectious burden, r(t) reveals the underlying epidemic trajectory, showing whether the disease pressure is building or being suppressed under the seed-treatment scenario.

Day 1 example: Zymoseptoria tritici under Scenario A (Systiva only)

Given initial conditions: $S_0 = 0.94, E_0 = 0.05, I_0 = 0.01, R_0 = 0$

Transmission at day 1, β(1): Using the exponential decay with environmental scaling,

$$\beta(1) = \beta_0 \cdot e^{-k \cdot t} \cdot f_{env}$$

with $\beta(1) = \beta_0 \cdot e^{-k \cdot t} \cdot f_{env} = 0.55 \cdot e^{-0.025 \cdot 1} \cdot 0.90$

$$\beta(1) = 0.55 \cdot e^{-0.025 \cdot 0.90} \approx 0.55 \cdot 0.9753 \cdot 0.90 \approx 0.482$$

Susceptible leaf area at day 1, S(1): Theoretical exponential hardening (for context):

$$S_{\text{theor}}(1) = S_0 \cdot e^{-d \cdot t} = 1.0 \cdot e^{-0.105} \approx 0.900$$

Empirical (from calibrated SEIR simulation used in the Table 1):

$$S_{\text{emp}}(1) = 0.72$$

Recovery rate at day 1, γ(1): Defined as inverse infectious period,

$$\gamma(1) = \frac{1}{D(1)} = \frac{1}{4.5} \approx 0.222$$

Epidemic growth rate at day 1, r(1): Using the SEIR-based indicator,

$$r(1) = \beta(1) \cdot S(1) - \gamma(1)$$

Substituting the empirical S(1),

$$r(1) = 0.482 \cdot 0.72 - 0.222 = 0.346 - 0.222 = 0.124$$

The positive value r(1) = 0.124 indicates that, on Day 1, transmission outweighs removal. In practical terms, the epidemic is expanding: Z. tritici continues to increase its infectious leaf area despite seed treatment.

Day 3 example: Zymoseptoria tritici under Scenario A (Systiva only)

Transmission rate β(3): From the table, the calibrated value is:

$$\beta(3) \approx 0.43$$

Susceptible leaf area S(3): Theoretical exponential decay:

$$S_{\text{theor}}(3) \approx 0.731$$

Empirical (field-calibrated SEIR simulation):

$$S_{\text{emp}}(3) = 0.65$$

Recovery rate γ(3): From the infectious period estimate (D≈4.1days),

$$\gamma(3) \approx 0.24$$

Epidemic growth rate r(3): Using the SEIR expression,

$$r(3) = \beta(3) \cdot S(3) - \gamma(3)$$

Substituting empirical values S(3),

$$r(3) = 0.43 \cdot 0.65 - 0.24 = 0.2795 - 0.24 \approx +0.055$$

For Day 3, the epidemic growth rate r(3) ≈ +0.055 is slightly positive, meaning transmission still outweighs removal. The infection continues to expand, consistent with the pathogen's latent-to-infectious transition.

For Day 5, it can be seen that the growth rate r(5) (approximately -0.007) is nearing zero and thus there is a change in direction; this indicates a point of transition. Transmission is now roughly equal to removal, resulting in a decrease in the rate of increase (growth) of the epidemic. On Day 7, the negative growth rate value r(7) is approximately -0.069 which indicates a period of suppression; at this point, removal is more prevalent than transmission. While the volume of infected tissue remains elevated, the velocity of the epidemic (momentum) has now begun to decline. On Day 10, suppression of the growth rate has increased significantly (r(10) = approximately -0.162), with removal being the dominant activity relative to transmission. Additionally, it is very clear that the trajectory of the epidemic has moved downward, but some level of infection burden still exists due to prior growth of the epidemic.

3.4 Sensitivity to parameter variation

Moderate variation in key epidemiological parameters produced predictable shifts in epidemic behavior without altering the qualitative conclusions of the model. Increasing the transmission rate β by 20% elevated the peak infectious leaf area and delayed the point at which r(t) became negative, consistent with a temporary strengthening of epidemic momentum. Conversely, reducing β accelerated suppression and lowered Imax.

Changes in the removal rate γ produced the opposite pattern: higher values of γ led to earlier transitions to r(t)<0, while lower values prolonged epidemic growth. Variations in the latent rate σ had comparatively smaller effects, influencing timing but not the overall shape of the epidemic curves.

Across all parameter sets, the sign of the epidemic growth rate remained fully consistent with the analytical threshold condition

$$r(t) = \beta(t)S(t) - \gamma(t)$$

confirming that the model's qualitative behavior is robust to moderate parameter uncertainty.

4 Discussion and Conclusions

The SEIR framework developed in this study provides a biologically grounded and dynamically responsive tool for simulating foliar disease progression in winter wheat during the critical BBCH 37 growth stage. By integrating pathogen traits, environmental modulation of transmission, and fungicide decay dynamics, the model captures realistic epidemic trajectories for P. tritici-repentis and Z. tritici under Mediterranean conditions.

Seed treatment with Systiva® (fluxapyroxad) effectively suppressed P. tritici-repentis during the early season, consistent with its known efficacy against necrotrophic pathogens. The addition of a foliar propiconazole application at BBCH 37 further enhanced disease suppression, producing uniformly negative epidemic growth rates r(t) and reduced infectious leaf area throughout the 10-day simulation period. This synergistic effect supports the principles of Integrated Disease Management and aligns with empirical findings from field trials in Thessaly, Greece. Three independent studies [1], [2], [19] reported reduced disease severity, improved canopy vigor, increased tiller density, and lower infection incidence under Systiva®-based programs, validating the modeled reductions in transmission rate β, increases in removal rate γ, and early suppression of r(t).

From a practical standpoint, the results highlight the importance of combining seed treatment with a foliar fungicide timed to canopy closure, a period characterized by microclimatic conditions favorable to foliar pathogen development. The contrasting responses of P. tritici-repentis and Z. tritici emphasize the need for pathogen-specific management strategies. Under seed treatment alone (Scenario A), Z. tritici maintained positive r(t) values beyond BBCH 37, reflecting its hemibiotrophic lifestyle and longer latent period, whereas P. tritici-repentis exhibited near-zero or slightly negative growth rates. When foliar propiconazole was added (Scenario B), both pathogens showed consistently negative r(t), demonstrating the enhanced suppression achieved through combined interventions. Table 3 further illustrates the added benefit of foliar fungicide application.

Recent applications of SEIR modeling in wheat pathosystems have demonstrated that integrating remote sensing with compartmental epidemic models can enhance regional disease forecasting accuracy, as shown for Fusarium head blight [40]. Such studies reinforce the value of dynamically structured models for capturing canopy-level disease processes under field conditions.

Environmental conditions strongly influenced epidemic development, as reflected in the differing prevalence patterns of the two pathogens. Similar modeling work on light leaf spot has shown that leaf wetness duration and temperature exert strong control over epidemic progress, reinforcing the importance of environmental forcing in disease development [41]. Z. tritici thrived under the warm and humid conditions typical of BBCH 37, meeting its moisture and temperature requirements for infection [25], [26]. The decline in r(t) under Scenario A reflects the duration of protection provided by seed treatment before fungicide decay reduced efficacy. Under Scenario B, the continued decline in r(t) demonstrates the capacity of foliar fungicides to suppress fungal growth even under favorable environmental conditions [27], [42]. The lower moisture requirements ofP. tritici-repentis explain its earlier suppression under seed treatment alone, further underscoring the importance of integrating environmental context into disease management decisions.

The epidemic growth rate r(t) emerges as a practical and interpretable metric for agronomists and farmers, offering a dynamic indicator of disease momentum and fungicide timing. Because r(t) reflects both pathogen biology and environmental modulation, it can support decision-making in integrated disease management programs for Mediterranean wheat systems.

Finally, the scenario analysis framework presented here enables exploration of additional factors such as cultivar resistance, canopy architecture, and pathogen race structure. Advances in molecular diagnostics and effector gene monitoring [43] can further refine predictive assessments, while long-term simulations incorporating climate variability can guide adaptive management strategies for Mediterranean and semi-arid wheat production.

Overall, this research provides a coherent and biologically informed framework for predicting foliar disease development at the leaf level. By integrating field data with epidemiological modeling, it supports more precise fungicide application and contributes to the ongoing refinement of sustainable, scientifically grounded approaches in plant disease management.

References:

[1] Vagelas I, Cavalaris C, Karapetsi L, Koukidis C, Servis, D, Madesis P, Protective effects of Systiva® seed treatment fungicide for the control of winter wheat foliar diseases caused at early stages due to climate change. Agronomy, 12(9), 2002. https://doi.org/10.3390/agronomy12092000

[2] Vagelas I, Efficacy of Systiva® seed treatment in managing tan spot and Septoria leaf blotch in winter wheat. Modern Concepts & Developments in Agronomy, 15(3), 2025, MCDA.000864. https://doi.org/10.31031/MCDA.2025.15.000864

[3] Bouras N, Kim Y M, Strelkov S E, Influence of water activity and temperature on growth and mycotoxin production by isolates of Pyrenophora tritici-repentis from wheat. International journal of food microbiology, 131 2-3, 2009, 251-5. DOI:10.1016/j.ijfoodmicro.2009.02.001

[4] Porras R, Miguel-Rojas C, Lorite I J, Pérez-de-Luque A, Sillero J C, Characterization of Durum Wheat Resistance against Septoria Tritici Blotch under Climate Change Conditions of Increasing Temperature and CO2 Concentration. Agronomy, 2023. DOI:10.3390/agronomy13102638

[5] Bartosiak S F, Arseniuk E, Szechyńska-Hebda M, Bartosiak E. Monitoring of Natural Occurrence and Severity of Leaf and Glume Blotch Diseases of Winter Wheat and Winter Triticale Incited by Necrotrophic Fungi Parastagonospora spp. and Zymoseptoria tritici. Agronomy, 11, 967, 2021. DOI:10.3390/AGRONOMY11050967

[6] Tissaoui S, Omri-Benyoussef N, Chaar H, Hassine M, Venisse J, Nasraoui B, Mougou-Hamdane A, Progression of wheat Tan spot under different bioclimatic stages and agricultural practices. Plant Protection Science, 2023. DOI:10.17221/103/2022-pps

[7] Robert C, Fournier C, Andrieu B, Ney B, Coupling a 3D virtual wheat (Triticum aestivum) plant model with a Septoria tritici epidemic model (Septo3D): a new approach to investigate plant-pathogen interactions linked to canopy architecture. Functional plant biology : FPB, 35 10, 2008, 997-1013. DOI:10.1071/FP08066

[8] Robert C, Garin G, Abichou M, Houlès V, Pradal C, Fournier, C, Plant architecture and foliar senescence impact the race between wheat growth and Zymoseptoria tritici epidemics. Annals of Botany, 121, 2018, 975–989. DOI:10.1093/aob/mcx192

[9] Abdullah A S, Gibberd M R, Hamblin J, Co-infection of wheat by Pyrenophora tritici-repentis and Parastagonospora nodorum in the wheatbelt of Western Australia. Crop and Pasture Science, 71, 2020, 119 - 127.DOI:10.1071/CP19412

[10] Colson E, Platz G J, Usher T R, Fungicidal control of Pyrenophora tritici-repentis in wheat. Australasian Plant Pathology, 32, 2003, 241-246. DOI:10.1071/AP03010

[11] Kildea S, Heick T, Hutton F, Bataille C, Aldén L, Kaneps J, Mäe A, Weigand S, Zajc J, Walker A S., Hellin P, Prevalence of key resistance alleles associated with DMI and SDHI fungicide resistance in European Zymoseptoria tritici populations in 2022. Journal of Plant Diseases and Protection, 132, 2025. DOI:10.1007/s41348-024-01049-y

[12] Heick TM, Justesen A F, Jørgensen L N, Anti-resistance strategies for fungicides against wheat pathogen Zymoseptoria tritici with focus on DMI fungicides. Crop Protection, 99, 2017, 108-117. DOI:10.1016/J.CROPRO.2017.05.009

[13] Lavrukaitė K, Almogdad M, Ramanauskienė J, Sabeckis A, Sensitivity of Lithuanian Zymoseptoria tritici to Quinone Outside Inhibitor and Succinate Dehydrogenase Inhibitor Fungicides. Agronomy, 2024. DOI:10.3390/agronomy14040813

[14] Birr T, Hasler M, Verreet J, Klink HTemporal Changes in Sensitivity of Zymoseptoria tritici Field Populations to Different Fungicidal Modes of Action. Agriculture, 2021. DOI:10.3390/AGRICULTURE11030269

[15] Vincent E M, Hill E M, Parnell S,Modelling the effectiveness of Integrated Pest Management strategies for the control of Septoria tritici blotch. PLOS Computational Biology, 21, 2025. DOI:10.1101/2025.02.28.639837

[16] Vagelas I, Important Foliar Wheat Diseases and their Management: Field Studies in Greece. Modern Concepts & Developments in Agronomy, 2021. DOI:10.31031/mcda.2021.08.000680

[17] Bazarra N, Colturato M, Fernández J R, Naso MG, Simonetto A, Gilioli G, Analysis of a Mathematical Model Arising in Plant Disease Epidemiology. Applied Mathematics & Optimization, 85, 2022. DOI:10.1007/s00245-022-09858-z

[18] Vagelas I, Effective strategies for managing wheat diseases: Mapping academic literature utilizing VOSviewer and insights from our 15 years of research. Agrochemicals, 4(1), 2025, 4. https://doi.org/10.3390/agrochemicals4010004

[19] Vagelas I, Sourlas A, Cavalaris C, SDHI fungicides: An important step in maintaining control of tan spot and Septoria leaf blotch diseases of wheat. Journal of Environmental Science, Sustainability, and Green Innovation, 1(2), 2025, 1–8. https://doi.org/10.63620/MKJESSGI.2025.1009

[20] Cunniffe N J, Laranjeira F F, Neri F M, DeSimone R E, Gilligan C A, Cost-Effective Control of Plant Disease When Epidemiological Knowledge Is Incomplete: Modelling Bahia Bark Scaling of Citrus. PLoS Computational Biology, 10, 2014. DOI:10.1371/journal.pcbi.1003753

[21] Cunniffe N J, Koskella B E, Metcalf C, Parnell S R, Gottwald T, Gilligan C A. Thirteen challenges in modelling plant diseases. Epidemics, 10, 2015, 6-10. DOI:10.1016/j.epidem.2014.06.002

[22] Abdullah F A, Liu F, Burrage P M, Burrage K, Li T, Novel analytical and numerical techniques for fractional temporal SEIR measles model. Numerical Algorithms, 79, 2017, 19 - 40. DOI:10.1007/s11075-017-0426-6

[23] AHDB, Practical measures to combat fungicide resistance in pathogens of wheat. Agriculture and Horticulture Development Board, 2023. https://ahdb.org.uk

[24] Baazeem A S, Nawaz Y, Arif M, Abodayeh K, AlHamrani M A, Modelling Infectious Disease Dynamics: A Robust Computational Approach for Stochastic SIRS with Partial Immunity and an Incidence Rate. Mathematics, (2023). DOI:10.3390/math11234794

[25] Miñana-Posada S, Feurtey A, Alassimone J, McDonald B A, Lorrain C, Responses to temperature shocks in Zymoseptoria tritici reveal specific transcriptional reprogramming and novel candidate genes for thermal adaptation. bioRxiv., 2024. https://doi.org/10.1101/2024.12.16.628617

[26] Boixel AL, Gélisse S, Marcel T C, Suffert F, Differential tolerance of Zymoseptoria tritici to altered optimal moisture conditions during the early stages of wheat infection. Journal of Plant Pathology, 104(1), 2022, 45–58. https://doi.org/10.1007/s42161-021-01025-7

[27] Mirzadi Gohari A, Ghiasi Noei F, Ebrahimi A, Ghanbari M A, Didaran F, Farzaneh M, Mehrabi R, Physiological and molecular responses of a resistant and susceptible wheat cultivar to the fungal wheat pathogen Zymoseptoria tritici. PLOS ONE, 19, 2024. DOI:10.1371/journal.pone.0308116

[28] Aguiar M, Van-Dierdonck J B, Stollenwerk N, Reproduction ratio and growth rates: Measures for an unfolding pandemic. PLoS ONE, 15, 2020. DOI:10.1101/2020.05.18.20105528

[29] Savary S, Nelson A, Willocquet L, Pangga I, Aunario J, Modeling and mapping potential epidemics of rice diseases globally. Crop Protection, 34, 2012, 6–17. https://doi.org/10.1016/j.cropro.2011.11.009

[30] Sparks A, Hijmans R, Savary S, Pangga I, Aunario J, epicrop: Simulation Modelling of Crop Diseases Using a Susceptible-Exposed-Infectious-Removed (SEIR) Model. doi:10.5281/zenodo.5070395, R package version 1.0.0.9000, 2022. https://codeberg.org/adamhsparks/epicrop.

[31] Bakare E A, Chakraverty S, Potucek R, Numerical Solution of an Interval-Based Uncertain SIR (Susceptible-Infected-Recovered) Epidemic Model by Homotopy Analysis Method. Axioms, 10, 114, 2021. DOI:10.3390/axioms10020114

[32] Prodanov D, Analytical solutions and parameter estimation of the SIR epidemic model. Mathematical Analysis of Infectious Diseases, 2022, 163 - 189. DOI:10.1016/B978-0-32-390504-6.00015-2

[33] Schippmann B, Burchard H, Rosenbrock methods in biogeochemical modelling – A comparison to Runge–Kutta methods and modified Patankar schemes. Ocean Modelling, 37, 2011, 112-121. DOI:10.1016/J.OCEMOD.2011.01.007

[34] Yilmaz F, Bakan H Ö, Weber G, Strong-order conditions of Runge-Kutta method for stochastic optimal control problems. Applied Numerical Mathematics, 157, 2020, 470-489. DOI:10.1016/j.apnum.2020.07.002

[35] Milne A, Paveley N, Audsley E, Livermore P, A wheat canopy model for use in disease management decision support systems. Annals of Applied Biology, 143(3), 2003, 265–274. https://doi.org/10.1111/j.1744-7348.2003.tb00295.x

[36] Derbyshire M C, Michaelson L V, Parker J, Kelly S, Thacker U, Powers S J, Bailey A, Hammond-Kosack K E, Courbot M, Rudd J J, Analysis of cytochrome b5 reductase-mediated metabolism in the phytopathogenic fungus Zymoseptoria tritici reveals novel functionalities implicated in virulence.

Fungal Genetics and Biology, 82, 2015, 69–84. https://doi.org/10.1016/j.fgb.2015.05.008

[37] Cox C M, Garrett K A, Bowden R L, Fritz A K, Dendy S P, Heer W F, Cultivar mixtures for the simultaneous management of multiple diseases: Tan spot and leaf rust of wheat. Phytopathology, 94(9), 2004, 961–969. https://doi.org/10.1094/PHYTO.2004.94.9.961

[38] Meile L, Carrasco-López C, Lorrain C, Kema GH, Saintenac C, Sánchez-Vallet A, The molecular dialogue between Zymoseptoria tritici and wheat. Molecular plant-microbe interactions : MPMI., 2024. DOI:10.1094/mpmi-08-24-0091-irw

[39] Hansen R, Fagundes W C, Stukenbrock E H, Comparative Transcriptomic and Microscopic Analyses of a Wild Wheat Relative Reveal Novel Mechanisms of Immune Suppression by the Pathogen Zymoseptoria tritici. Molecular plant-microbe interactions : MPMI, 2025. DOI:10.1094/MPMI-11-24-0147-R

[40] Xiao Y, Dong Y, Huang W, Liu L. Regional prediction of Fusarium head blight occurrence in wheat with remote sensing based Susceptible-Exposed-Infectious-Removed model. Int. J. Appl. Earth Obs. Geoinformation, 114, 2022, 103043. DOI:10.1016/j.jag.2022.103043

[41] Papastamati K, Welham SJ, Fitt BD, Gladders P. Modelling the progress of light leaf spot (Pyrenopeziza brassicae) on winter oilseed rape (Brassica napus) in relation to leaf wetness and temperature. Plant Pathology, 50, 2001,154-164. DOI:10.1046/J.1365-3059.2001.00551.X

[42] Sparks C A, Jørgensen L N, Matzen N, Heick T M, O'Driscoll A, Clark B, Waite K, Blake J, Glazek M, Maumene C, Couleaud G, Rodemann B, Weigand S, Bataille C, Bán R, Hellin P, Kildea S, Stammler G, Shifting sensitivity of Septoria tritici blotch compromises field performance and yield of main fungicides in Europe. Frontiers in Plant Science, 13, 2022. 1060428. https://doi.org/10.3389/fpls.2022.1060428

[43] Kamel S, Cherif M, Hafez M, Despins T, Aboukhaddour R, Pyrenophora tritici–repentis in Tunisia: Race Structure and Effector Genes. Frontiers in Plant Science, 10, 2019. DOI:10.3389/fpls.2019.01562

Contribution of Individual Authors to the Creation of a Scientific Article (Ghostwriting Policy)

Ioannis Vagelas, defined the methodology, gathered the data, analyzed and writing the paper.

Sources of Funding for Research Presented in a Scientific Article or Scientific Article Itself

No funding was received for conducting this study.

Conflict of Interest

The author has no conflicts of interest to declare that are relevant to the content of this article.